Magnetocaloric Properties of Melt-Spun Fe–Ni–Mn–Ga Ribbons

C. W. Shih[1], X. G. Zhao[2], H. W. Chang[3], Y. C. Tseng[4], and W. C. Chang[1]

[1]Department of Physics, National Chung Cheng University, Chia-Yi, 621 Taiwan, ROC
[2]Shenyang National Laboratory for Materials Science, Institute of Metal Research, Chinese Academy of Sciences, Shenyang 110016, China
[3]Department of Applied Physics, Tunghai University, Taichung, Taiwan, ROC
[4]Department of Materials Science and Engineering, National Chiao Tung University, Hsin-chu 30010, Taiwan, ROC

The effects of Ni substitution for Fe on phase constitutions, Curie temperature T_C, and magnetocaloric properties of melt-spun $Fe_{50-x}Ni_xMn_{25}Ga_{25}$ (x =0, 1, 3, 5 and 7) ribbons have been investigated. X-ray diffraction results show that the main phase in the $Fe_{50-x}Ni_xMn_{25}Ga_{25}$ (x = 0-7) alloy changed with the increase of Ni content from FCC structure for x = 0 into B2 structure for x = 1-7. Besides, the magnetic phase exhibits phase transition of ferromagnetic into paramagnetic state with increasing temperature for the samples with B2-type structure. The Curie temperature T_C of these ribbons varies in the temperature range of 232-257 K. The peak values of the maximal magnetic entropy change, $-\Delta S_M{}^{max}$, are about 1.4-1.6 Jkg/K for Ni-substituted ribbons at a maximum applied field of 30 kOe. On the other hand, the relatively broader temperature range at the half maximum of ΔS_M peak ($\sim$ 90 K), low-cost and nontoxic elements make Fe–Ni–Mn–Ga-based ribbons the promising candidates for magnetic refrigeration applications close to room temperature.

Index Terms—**Heusler alloy, magnetocaloric properties, melt-spun ribbon.**

I. Introduction

SINCE a large magnetic field-induced strain (MFIS) associated with a rearrangement of martensite variants by an external magnetic field in Ni–Mn–Ga alloys was first reported in 1996, [1] ferromagnetic shape memory alloys (FSMAs) have attracted significant attention due to their interesting physical properties, such as large magnetic-field-induced strain, [1], [2] giant magnetocaloric effects (MCEs), [3], [4] large magnetoresistance (MR), [5], [6] and exchange bias (EB) behavior [7], [8]. These properties make them a promising candidate as potential material for various practical applications in the field of smart, magnetic refrigeration and spintronics.

In contrast to most developed Ni–Mn based Heusler alloys, another representative of the FSMAs, i.e., Fe–Mn based system, has not received much attention up to now, such as Fe–Mn–Ga alloys, which also possess many of the above-mentioned features. Recently, Zhu *et al.* have reported that for a slightly off-stoichiometric $Fe_{50}Mn_{22.5}Ga_{27.5}$ alloy, a field-induced transformation from a paramagnetic (PM) parent phase to a ferromagnetic (FM) martensite phase takes place at 163 K (on cooling), leading to a large lattice distortion of 33.5%; in the meantime, a large shape memory strain up to about 3.6% is observed due to the martensite transformation (MT) [9]. On the other hand, the giant EB effect was observed in stoichiometric Fe_2MnGa alloy ribbon, because transformation from antiferromagnetic (AFM) to FM phase can be induced by applying a magnetic field or by changing the temperature. In addition, the EB behavior and enhanced coercivity occur simultaneously, revealing an exchange coupling between the coexisting antiferromagnetic and ferromagnetic phase [10], [11].

In our previous work, we reported phase transformation and EB behavior in as-spun Fe–Mn–Ga ribbons [12]. However, to date, there is no report on the effect of other magnetic elements' (Co or Ni) addition on the structure and magnetic phase evolution of Fe–Mn–Ga melt-spun ribbon systems. In this present work, the effect of Ni substitution for Fe on the crystal structure, magnetic state and magnetocaloric effect of the Fe–Ni–Mn–Ga Heusler alloy ribbons are reported.

II. Experiment

The alloys with the nominal composition of $Fe_{50-x}Ni_xMn_{25}Ga_{25}$ (x =0, 1, 3, 5 and 7) were prepared using arc melting pure elements ($>$ 99.9%) in a high-purity argon atmosphere. To compensate for Mn losses during processing, an excess of 6 wt.% Mn was added. The ingot was melted three times to ensure homogeneity, and then melt-spun with a single-roll melt-spinner at a wheel linear speed of 15 m/s. The crystal structure of the ribbons was identified by X-ray diffraction (XRD) using Cu-$K\alpha$ radiation at room temperature. Magnetic measurements were performed in the temperature interval of 10 $-$ 330 K, and in external magnetic fields up to 30 kOe, using a physical properties measuring system (PPMS, Quantum Design Inc.) platform with a vibrating sample magnetometer module. The magnetic field was applied along the ribbon plane direction. Zero-field-cooled (ZFC) and field-cooled (FC) thermomagnetic curves were recorded at 200 Oe with a temperature heating or cooling rate of 10 K/min. Magnetic phase transition temperature was inferred from the maximum or minimum in the dM/dT versus T curve. The maximum magnetic entropy changes ΔS_M (T, H)

Manuscript received May 05, 2013; revised July 17, 2013; accepted July 24, 2013. Date of current version December 23, 2013. Corresponding author: W. C. Chang (e-mail:phywcc@ccu.edu.tw).

Color versions of one or more of the figures in this paper are available online at http://ieeexplore.ieee.org.

Digital Object Identifier 10.1109/TMAG.2013.2276091

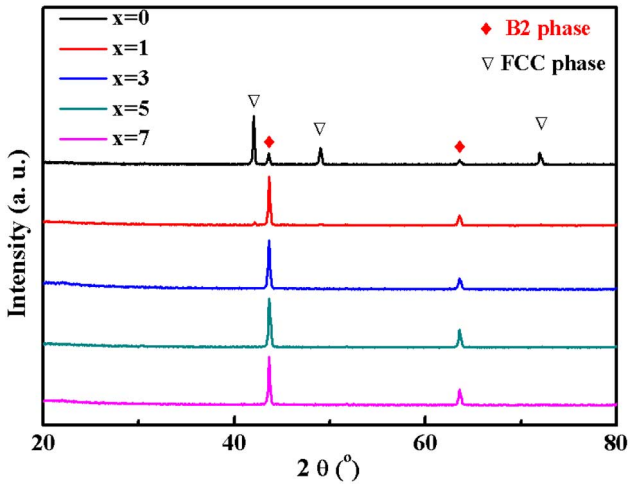

Fig. 1. XRD patterns of the melt spun $Fe_{50-x}Ni_xMn_{25}Ga_{25}$ (x =0, 1, 3, 5 and 7) ribbons at room temperature.

were calculated from isothermal magnetization curves using the Maxwell relation [13]

$$\Delta S_M(T,H) = \int_0^H \left(\frac{\partial M}{\partial T}\right)_H dH.$$

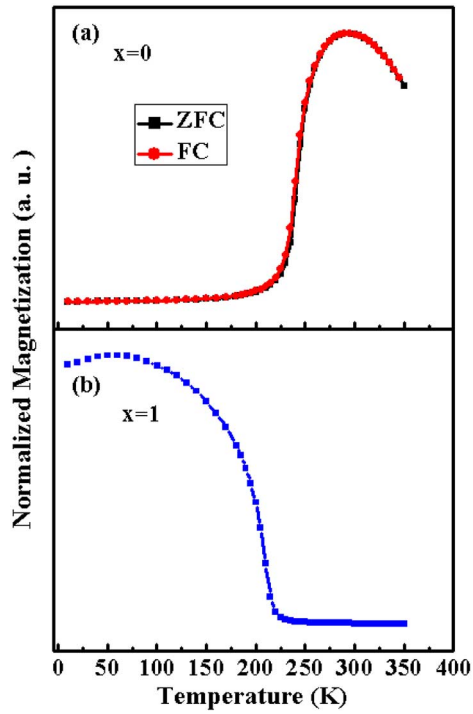

Fig. 2. (a) ZFC and FC magnetization curves as a function of temperature of $Fe_{50}Mn_{25}Ga_{25}$ and (b) of $Fe_{49}Ni_1Mn_{25}Ga_{25}$ ribbons obtained at a field of 200 Oe.

III. Results and Discussion

Fig. 1 shows XRD patterns of the as-spun $Fe_{50-x}Ni_xMn_{25}Ga_{25}$ (x =0, 1, 3, 5 and 7) ribbons at room temperature. The crystal structure of these series ribbons includes two kinds of structures, an ordered face-center-cubic (fcc) lattice of $L1_2$-type (Cu_3Au) for x = 0 and a partially ordered B2 phase for x = 1-7, respectively. According to the results of previous reports, stoichiometric Fe_2MnGa alloy should have the stable $L2_1$-type of structure [14]. However, it was experimentally found that stoichiometric Fe_2MnGa alloy crystallizes in a fcc-type structure [9], [10], [15]. Theoretical results reported by Kudryavtsev *et al.* [16] showed that the $L2_1$-type crystal structure with a lattice constant of a = 0.57 nm in Fe_2MnGa is stable with ferrimagnetic order, instead of FM order. On the other hand, stable ordered fcc-type structure with lattice constants of a = 0.3644 nm and a = 0.3666 nm exhibited ferromagnetic and ferrimagnetic order, respectively. In this work, for x = 0 samples, the main phase is found ordered fcc lattice of $L1_2$-type (Cu_3Au), implying that the structure of ordered fcc-type is more stable than $L2_1$-type in Fe_2MnGa alloy. However, for alloy ribbons with x > 1, the main phase of ribbons changes into B2 structure. It is presumed that a chemical disorder B2 phase favors to form due to Ni-added alloy systems consisting of more than three elements [17] and also rapid solidification process.

Fig. 2 shows zero-field cooled (ZFC) and field-cooled (FC) magnetization as a function of temperature $M(T)$ of $Fe_{50-x}Ni_xMn_{25}Ga_{25}$ ribbons with x =0 and 1. It is seen that the behaviors of these two curves are quite different. For x = 0, a sudden jump in magnetization with increasing temperature is observed. In addition, the magnetization curves recorded in field-cooled and field-warmed procedures are almost overlapped around the magnetic phase transition, indicating the second-order nature of the magnetic transitions. The structure and magnetic phase transition of the ribbons with x = 0 are consistent with previous work [12], that is, magnetic phase transition of fcc structure from antiferromagnetic (AFM) to FM with increasing temperature. For Ni-added ribbons with x = 1, it exhibits a magnetic phase transition at T_C = 232 K, which corresponds to Curie temperature of B2-type phase change from FM to PM state.

The temperature dependence of magnetization $M(T)$ curves of $Fe_{50-x}Ni_xMn_{25}Ga_{25}$ (x = 1-7) ribbons, measured in an applied field of 1 kOe and temperature range from 190 to 380 K, are shown in Fig. 3(a), and their corresponding dM/dT-versus-T curves are shown in Fig. 3(b). The Curie temperature T_C values, obtained from the M–T curves, are summarized in Table I. From the results of Fig. 3, it can be found that the T_C and magnetization of B2 phase are increased with increasing Ni concentration. In B2-type structure, the magnetic moments depend mainly on anti-parallel coupling of Mn atoms and Fe atoms. Hence, a part of Fe replaced by Ni might reduce the exchange coupling of Fe and Mn atoms, leading to the enhancement of magnetization and Curie temperature.

The isothermal magnetization curves for $Fe_{50-x}Ni_xMn_{25}Ga_{25}$ (x = 1-7) ribbons are measured with an increasing magnetic field in a wide temperature range. The MCE as a function of temperature and magnetic field was calculated from the isothermal magnetization curves using the Maxwell relation under 0-30 kOe magnetic field changes. The M-H curves of representative $Fe_{49}Ni_1Mn_{25}Ga_{25}$ ribbons

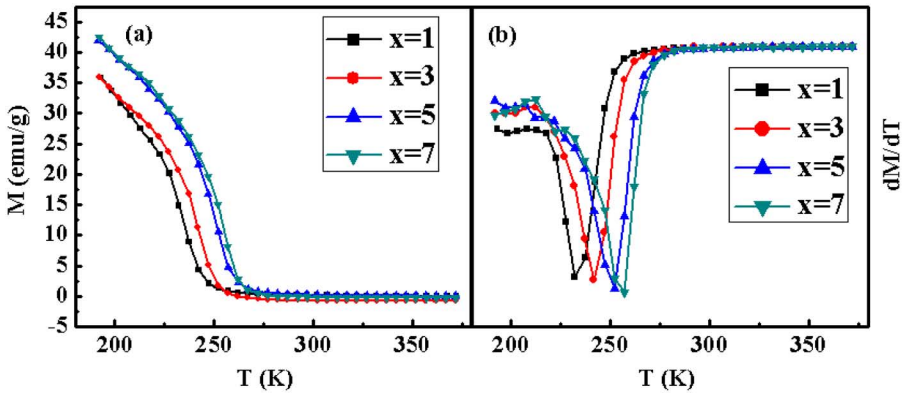

Fig. 3. Magnetization curves as a function of temperature of $Fe_{50-x}Ni_xMn_{25}Ga_{25}$ (x =1, 3, 5, 7) ribbons obtained at a field of 1 kOe. (b) Corresponding $dM/dT(T)$ curves.

TABLE I
NOMINAL COMPOSITION, CURIE TEMPERATURE OF MAGNETIC PHASE TRANSITION (T_C), MAXIMAL MAGNETIC ENTROPY CHANGES, ($-\Delta S_M{}^{max}$) AND RELATIVE COOLING POWER (RCP) AT MAGNETIC FIELD CHANGE OF 30 KOE OF $Fe_{50-x}Ni_xMn_{25}Ga_{25}$ RIBBONS

X	Nominal composition	T_C (K)	$-\Delta S_M{}^{max}$ (Jkg/K)	RCP (Jkg)
1	$Fe_{49}Ni_1Mn_{25}Ga_{25}$	232	1.6	147.2
3	$Fe_{47}Ni_3Mn_{25}Ga_{25}$	242	1.4	126
5	$Fe_{45}Ni_5Mn_{27}Ga_{23}$	252	1.5	135
7	$Fe_{43}Ni_7Mn_{27}Ga_{23}$	257	1.5	130.5

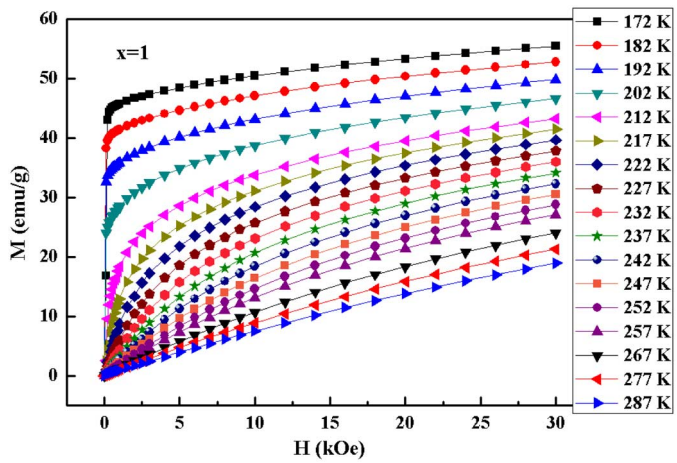

Fig. 4. Isothermal magnetization curves of $Fe_{49}Ni_1Mn_{25}Ga_{25}$ ribbons obtained for a field change of 30 kOe.

obtained for a field change of 30 kOe are shown in Fig. 4. The maximal magnetic entropy changes of $-\Delta S_M$, as a function of Ni content x, are listed in Table I. The Ni substitution alters the magnetocaloric properties around the transition temperatures. The peak values of the maximal magnetic entropy changes, $-\Delta S_M{}^{max}$, are about 1.4-1.6 Jkg/K for Ni-substituted ribbons, at a maximum applied field of 30 kOe. The change in $-\Delta S_M$ should be caused by a change of magnetization around the transition temperatures. The difference in the magnetization can be ascribed to the exchange interaction on the magnetic moments of Fe and Mn atoms in Ni–Mn-based alloys. Hence, any change of the positions in B2 lattices caused by Ni addition could modify the strength of the interactions, leading to different magnetic exchanges in the phases, resulting in the change of magnetic entropy changes $-\Delta S_M$ and T_C.

Another important parameter for magnetic refrigeration is the refrigeration capacity (RC), which is measured in literature by different methods [18]. The RC value represents how much heat can be transferred between cold and hot sinks in an ideal refrigerant cycle, [18] which is of practical significance. In present work, the RC values are estimated using the relative cooling power (RCP), which is given by the product of the $\Delta S_M(T)$ maximum ($\Delta S_M{}^{max}$) and full width at half maximum of $\Delta S_M{}^{max}$ (δT_{FWHM}), i.e., RCP = $-\Delta S_M{}^{max} \times \delta T_{FWHM}$. The RCP is approximately 4/3 times larger than the cooling capacity for the same temperature interval. The RCP values for each of the ΔS_M peaks of $Fe_{50-x}Ni_xMn_{25}Ga_{25}$ (x = 1-7) ribbons are also listed in Table I. The values of the RCP for $Fe_{50-x}Ni_xMn_{25}Ga_{25}$ (x = 1-7) ribbon samples are located in the range of 126-147.2 Jkg for a magnetic field change of 30 kOe, which is much larger than those of iron-based $Fe_{60}Cr_{14}Nb_3Si_{13}B_9Cu_1$ alloy (87.3 Jkg) [19]. Therefore, despite relatively lower peak values of $-\Delta S_M$, but the relatively broader temperature range of the half maximum of ΔS_M peak ($\sim$ 90 K), low-cost, nontoxic elements and simple synthesis procedures still make Fe–Ni–Mn–Ga-based ribbons promising candidates for magnetic refrigeration applications close to room temperature.

IV. CONCLUSION

The effect of Ni substitution for Fe in $Fe_{50-x}Ni_xMn_{25}Ga_{25}$ (x = 0-7) ribbons on the structure, magnetic phase transition and magnetocaloric properties has been reported. The experimental results show that the main phase of ribbons is changed with Ni concentration from the ordered fcc structure for x = 0 into B2-type structure for x = 1-7. A proper addition of Ni can improve the magnetic coupling between magnetic atoms, leading to enhanced both magnetization and Curie

temperature. The maximum values of the magnetic entropy changes -$\Delta S_M{}^{max}$ are 1.6, 1.4, 1.5 and 1.5 J/kg K at 232, 242, 252 and 257 K for x = 1, 3, 5, and 7, respectively, under applied magnetic field of 30 kOe. The moderate ΔS_M and RCP values and low cost elements suggest that $Fe_{50-x}Ni_xMn_{25}Ga_{25}$ (x = 1-7) ribbons may be promising substances for magnetic refrigeration materials working in the temperature interval range of $200 - 300$ K.

ACKNOWLEDGMENT

This paper was supported by National Science Council, Taiwan, under Grant NSC-101-2112-M-194-005-MY3.

REFERENCES

[1] K. Ullakko, J. K. Huang, C. Kantner, R. C. O'Handley, and V. V. Kokorin, "Large magnetic-field-induced strains in Ni_2MnGa single crystals," *Appl. Phys. Lett.*, vol. 69, no. 13, pp. 1966–1968, 1996.

[2] R. Kainuma, Y. Imano, W. Ito, Y. Sutou, H. Morito, S. Okamoto, O. Kitakami, K. Oikawa, A. Fujita, T. Kanomata, and K. Ishida, "Magnetic-field-induced shape recovery by reverse phase transformation," *Nature*, vol. 439, no. 7079, pp. 957–960, 2006.

[3] Z. D. Han, D. H. Wang, C. L. Zhang, H. C. Xuan, B. X. Gu, and Y. W. Du, "Low-field inverse magnetocaloric effect in $Ni_{50-x}Mn_{39+x}Sn_{11}$ Heusler alloys," *Appl. Phys. Lett.*, vol. 90, no. 4, p. 042507, 2007.

[4] V. K. Sharma, M. K. Chattopadhyay, K. H. B. Shaeb, A. Chouhan, and S. B. Roy, "Large magnetoresistance in $Ni_{50}Mn_{34}In_{16}$ alloy," *Appl. Phys. Lett.*, vol. 89, no. 22, p. 222509, 2006.

[5] S. Y. Yu, Z. X. Cao, L. Ma, G. D. Liu, J. L. Chen, G. H. Wu, B. Zhang, and X. X. Zhang, "Realization of magnetic field-induced reversible martensitic transformation in NiCoMnGa alloys," *Appl. Phys. Lett.*, vol. 91, no. 10, p. 102507, 2007.

[6] K. Koyama, H. Okada, K. Watanabe, T. Kanomata, R. Kainuma, W. Ito, K. Oikawa, and K. Ishida, "Observation of large magnetoresistance of magnetic Heusler alloy $Ni_{50}Mn_{36}Sn_{14}$ in high magnetic fields," *Appl. Phys. Lett.*, vol. 89, no. 18, pp. 182510–182513, 2006.

[7] M. Khan, I. Dubenko, S. Stadler, and N. Ali, "Exchange bias behavior in Ni–Mn–Sb heusler alloys," *Appl. Phys. Lett.*, vol. 91, no. 7, p. 072510, 2007.

[8] M. Khan, I. Dubenko, S. Stadler, and N. Ali, "Exchange bias in bulk Mn rich Ni–Mn–Sn Heusler alloys," *J. Appl. Phys.*, vol. 102, no. 11, p. 113914, 2007.

[9] W. Zhu, E. K. Liu, L. Feng, X. D. Tang, J. L. Chen, G. H. Wu, H. Y. Liu, F. B. Meng, and H. Z. Luo, "Magnetic-field-induced transformation in FeMnGa alloys," *Appl. Phys. Lett.*, vol. 95, no. 22, p. 222512, 2009.

[10] X. D. Tang, W. H. Wang, W. Zhu, E. K. Liu, G. H. Wu, F. B. Meng, H. Y. Liu, and H. Z. Luo, "Giant exchange bias based on magnetic transition in gamma-Fe_2MnGa melt-spun ribbons," *Appl. Phys. Lett.*, vol. 97, no. 24, p. 242513, 2010.

[11] X. D. Tang, W. H. Wang, G. H. Wu, F. B. Meng, H. Y. Liu, and H. Z. Luo, "Tuning exchange bias by thermal fluctuation in $Fe_{52}Mn_{23}Ga_{25}$ melt-spun ribbons," *Appl. Phys. Lett.*, vol. 99, no. 22, p. 222506, 2011.

[12] C. W. Shih, X. G. Zhao, H. W. Chang, W. C. Chang, and Z. D. Zhang, "The phase evolution, magnetic and exchange bias properties in $Fe_{50}Mn_{24+x}Ga_{26-x}$ (x = 0 – 3) melt-spun ribbons," *J. Alloys Compounds*, vol. 570, no. 0, pp. 14–18, 2013.

[13] K. A. Gschneidner and V. K. Pecharsky, "Magnetocaloric materials," *Annu. Rev. Mater. Sci.*, vol. 30, no. 1, pp. 387–429, 2000.

[14] A. T. Zayak, P. Entel, K. M. Rabe, W. A. Adeagbo, and M. Acet, "Anomalous vibrational effects in nonmagnetic and magnetic heusler alloys," *Physical Rev. B.*, vol. 72, no. 5, p. 054113, 2005.

[15] T. Gasi, A. K. Nayak, M. Nicklas, and C. Felser, "Structural and magnetic properties of the heusler compound Fe_2MnGa," *J. Appl. Phys.*, vol. 113, no. 17, pp. 17E301–17E303, 2013.

[16] Y. V. Kudryavtsev, N. V. Uvarov, V. N. Iermolenko, I. N. Glavatskyy, and J. Dubowik, "Electronic structure, magnetic and optical properties of heusler alloy," *Acta Materialia*, vol. 60, no. 12, pp. 4780–4786, 2012.

[17] A. Inoue, "High strength bulk amorphous alloys with low critical cooling rates," *Japan Inst. Metals*, vol. 36, no. 7, pp. 866–875, 1995.

[18] K. A. Gschneidner, Jr., Jr., V. K. Pecharsky, A. O. Pecharsky, and C. B. Zimm *et al.*, "Recent developments in magnetic refrigeration," *Mater. Sci. Forum*, vol. 315, p. 69, 1999.

[19] S. Atalay, H. Gencer, and V. S. Kolat, "Magnetic entropy change in $Fe_{74-x}Cr_xCu_1Nb_3Si_{13}B_9$ (x = 14 and 17) amorphous alloys," *J. Non-Crystalline Solids*, vol. 351, no. 30–32, pp. 2373–2377, 2005.